Advances in Science and Technology Research Journal

Advances in Science and Technology Research Journal, 2025, 19(9), 292–309
https://doi.org/10.12913/22998624/207426
ISSN 2299-8624, License CC-BY 4.0

Received: 2025.06.22
Accepted: 2025.07.15
Published: 2025.08.01

Structural and surface characterization of adsorbents applied in liquid chromatography

Regina Lech-Przywara[1*], Tomasz Galek[2], Mateusz Przywara[3], Lidia Zapała[4], Wojciech Zapała[3]

[1] Doctoral School of the Rzeszow University of Technology, al. Powstańców Warszawy 12, 35-959 Rzeszów, Poland
[2] Department of Integrated Design and Tribology Systems, Faculty of Mechanics and Technology, Rzeszow University of Technology, ul. Kwiatkowskiego, 37-450 Stalowa Wola, Poland
[3] Department of Chemical and Process Engineering, Faculty of Chemistry, Rzeszow University of Technology, al. Powstańców Warszawy 6, 35-959 Rzeszów, Poland
[4] Department of Inorganic and Analytical Chemistry, Faculty of Chemistry, Rzeszow University of Technology, al. Powstańców Warszawy 6, 35-959 Rzeszów, Poland
* Corresponding authors' e-mail: d555@stud.prz.edu.pl, ichwz@prz.edu.pl

ABSTRACT

A detailed analysis of the four commercial stationary phases often applied in liquid chromatography was performed using the following: SEM-EDS techniques and specific surface area and porosity analysis methods (multipoint BET, BJH, DH and DFT). The SEM-EDS results confirmed that the main component of all adsorbents examined is silica (SiO_2), while differences in oxygen content indicate varied approaches to surface modification, ranging from the strongly hydrophilic phase of TSK Gel Amide-80 to the hydrophobic Nucleodur C18 Gravity. Besides, the presence of trace amounts of metals may influence the additional analyte-adsorbent interaction of different nature. A comparison of specific adsorbent surface area data obtained using the multipoint BET method with the manufacturers values revealed significant discrepancies in the cases of TSK Gel Amide 80 and Nucleodur C18 Gravity, which may be the result of differences in pore accessibility and measurement methods. However, the Eurospher II 100-5 HILIC and Purospher STAR NH_2 phases showed good agreement with the manufacturers data. The porous structure of the phase studied shows significant differences: TSK Gel Amide 80 is characterized by mesopores with a uniform distribution, which favor the retention of larger molecules; Eurospher II 100-5 HILIC is microporous and selective for small, polar analytes; Nucleodur C18 Gravity has a structure typical of reversed phase materials; and Purospher STAR NH_2 exhibits the highest porosity, which favors the retention of large molecules, although it can also lead to the retention of undesirable analytes.

Keywords: adsorbent, liquid chromatography, SEM-EDS, multipoint BET, porosity.

INTRODUCTION

Liquid chromatography is one of the key separation techniques used in the qualitative and quantitative analysis of complex chemical mixtures. This process is also increasingly used to separate compounds from of the different mixtures on an industrial scale. Due to its high sensitivity and selectivity, it is widely used in various fields, including pharmaceutical, biochemical, environmental and other, also industrial applications. A critical factor determining the efficiency of this process is the use of adequate adsorbents as the stationary phase, which defines the retention/sorption mechanism. The structural parameters of the materials used as stationary phases, such as the specific surface area, the pore size distribution and volume, the morphology and the chemical nature of the surface directly influence the interactions between the analytes and the

adsorbent surface. Furthermore, mass transport phenomena and dispersion processes within the flow system must be considered, as they play a key role in shaping and determining the width of chromatographic peaks. The complex interplay between the porous structure of the adsorbent, the physicochemical properties of the analytes, and the operating conditions of chromatography affects the overall separation efficiency, which makes the characterization of stationary phases the subject of extensive scientific research [1, 2].

Contemporary research on liquid chromatography, particularly in the context of mass transport mechanisms, diffusion, and dispersion, emphasizes the critical importance of thoroughly understanding the structure of adsorbents in the separation process. As mentioned above, the structure of adsorbents including their morphology, specific surface area, pore volume, and pore size distribution plays a key role in determining mass transport mechanisms within the chromatographic column. A high specific surface area, resulting from the presence of numerous pores of varying sizes (micro-, meso- and macropores), promotes effective adsorption of analytes by increasing the number of available interaction sites, which translates into improved separation resolution. However, a complex and often irregular surface structure may simultaneously act as a barrier to the free flow of the mobile phase and analytes. In such cases, analyte molecules must overcome various diffusion resistances, both in the interparticle space and within the internal pore structure of the adsorbent, leading to a reduction in the mass transport rate. In practice, this means that the more intricate and developed the material structure, the greater the overall diffusion resistance, which can result in broadened chromatographic peaks, reduced detection sensitivity, and decreased separation resolution [3–6].

The pore size distribution is a crucial factor that influences the efficiency of mass transport in chromatographic systems. Porosity that encompasses a wide range of sizes – from micropores to macropores – can lead to uneven flow of the mobile phase, resulting in the formation of zones with different diffusion velocities. This variation causes local differences in the retention times of the analyte, which consequently affects the width and symmetry of the chromatographic peaks. Small pores, while increasing the total specific surface area of the adsorbent, can create very narrow channels that hinder the free flow of molecules and increase the resistance to transport. These limitations favor what is known as pore diffusion, which occurs more slowly than diffusion in the mobile phase, delaying the transport of analytes and leading to peak broadening over time. On the other hand, larger pores provide better access to the internal space and facilitate the migration of molecules, promoting faster transport and more favorable peak profiles. Such structural heterogeneity of the pore system directly affects the dispersion phenomenon – the spread of molecules in the mobile phase – which is critical for assessing the quality of separation. The greater the dispersion, the lower the resolution and analytical precision of the method [7–9].

The mass transport mechanisms in a chromatographic column result from a complex combination of molecular diffusion and convective flow of the mobile phase. Molecular diffusion, occurring at the microscale level, is responsible for the spreading of analyte molecules within the pores of the adsorbent, where convective flow ensures movement of the mobile phase through the column, enabling the transport of analytes. The detailed mathematical analysis of the mass transport phenomena in chromatography is described in detail in the available literature (e.g. [10–18]). A very important factor is also dispersion. Dispersion is primarily the result of differences in the diffusion velocities of analyte molecules in different parts of the column. When a band migrates along a column packed with e.g. adsorbent particles, it spreads axially because of the combination effects of axial diffusion and the inhomogeneity of the pattern of flow velocity in a packed bed (this phenomenon is particularly noticeable in the case of porous materials, often with an irregular pore structure, where molecules can move along different paths at varying speeds). In this case we are dealing with the axial dispersion. This combination of effects is accounted for by a single term – so called the axial dispersion coefficient. It is independent of the mass transfer resistance and of the other contributions of kinetic origin to band broadening. To a large extent, it participates in mass transfer processes and influences the ability of a material to adsorb substances. The greater the dispersion, the more spread out the shapes of the chromatographic peaks, leading to a decrease in the separation resolution. In porous beds (e.g. in chromatographic columns), axial dispersion can be expressed by the so called axial Peclet number, *Pe,* [18]:

$$Pe = \frac{u \cdot L}{D_L \cdot \varepsilon_e} \quad (1)$$

where: u – mean linear velocity of mobile phase flow (cm/s), L – column length (cm), D_L – axial dispersion coefficient (cm²/s), ε_e – the external (or interparticle or interstitial) porosity, which is the fractional volume of the cavities in the bed that are between and around the particles.

The height equivalent to a theoretical plate, H - Eq.(2), is a parameter that describes the efficiency of a chromatographic column – the smaller the value of H, the more efficient the separation of analytes [12, 16–18]:

$$H = \frac{L}{Pe} \quad (2)$$

It can be interpreted as the length of the column segment where the theoretical separation of substances occurs. A high value of H indicates strong dispersion and loss of resolution, while a low value signifies well-optimized flow and minimization of analyte band-broadening phenomena.

In addition, interactions between analytes and the adsorbent can be modified through chemical surface modification, which affects both the adsorption efficiency and mass-transport mechanisms. For example, the introduction of specific functional groups, such as hydroxyl, amino, or carboxyl groups, increases the affinity of the adsorbent for selected compounds, enhancing interactions between the adsorbent and the analyte. Such modifications can also subtly alter the nature of pores – for instance, by changing their polarity – which affects the diffusion of molecules within the adsorbent structure, facilitating or restricting their transport. This allows for precise adjustment of material properties to a specific chromatographic application, resulting in improved selectivity and separation efficiency [6, 19–20]. The availability of data provided by manufacturers and presented in the literature regarding the characteristics of the adsorbents used is limited; therefore a detailed characterization of adsorbents seems to be very important. Research of this type was the main goal of our work. Our investigations included both the study of the different adsorbent surface structure using advanced microscopic techniques (e.g. SEM-EDS) and the evaluation of pore distribution and measurement of specific surface area (e.g., using the multipoint BET, BJH, DH, DFT methods), which is an essential tool in optimizing chromatographic processes. This analysis allows identification of key relationships between the microstructure of the adsorbents and the mass transport mechanisms, allowing the precise matching of the materials with specific analytical requirements [21–23].

MATERIALS AND METHODS

Materials

In this article, four commercial adsorbents were used for the studies (Table 1). These adsorbents (from the columns listed in Table 1) were selected for their different adsorption properties and their wide and different practical applications in liquid chromatography. Table 1 also presents the column parameters declared by the manufacturer.

Methodology of study

Microanalysis SEM-EDS of stationary phases

The SEM-EDS (scanning electron microscopy with energy dispersive X-ray spectroscopy) method is an analytical technique used for detailed analysis of the morphology of samples and their chemical composition. In this method, a scanning electron microscope (SEM) is used to obtain high-resolution images of the surface of the samples, and then an energy dispersive X-ray spectrometer (EDS) allows for precise chemical analysis by measuring the energy of X-ray photons emitted from the sample, which

Table 1. The parameters of the chromatographic columns under investigation, as declared by the manufacturer

Chromatographic columns	Adsorbent designation	Filling structure	Column dimensions [mm]	Mean particle diameter [µm]	Specific surface area [m²/g]
TSK Gel Amide-80	A	amide	4.6 × 100	5	450
Eurospher II 100-5 HILIC	B	dipolar	4.6 × 150	5	320
Nucleodur C18 Gravity	C	C-18	4.0 × 125	5	338
Purospher STAR NH_2	D	amine	4.6 × 125	5	330

allows the identification of the chemical elements present in the analyzed sample [21, 24, 25]. In the conducted studies, a TESCAN MIRA3 SEM microscope equipped with an Oxford Instruments X-MaxN EDS spectrometer was used. The analyses were performed with an accelerating voltage of 20 keV, which provided the necessary resolution and accuracy to obtain SEM images and EDS analysis. The working distance was set to 15 mm. During the analysis, the samples were placed on aluminum stubs covered with carbon tape, which was visible as a black background in the SEM images. To obtain SEM images,, we used a back scattered electron (BSE) detector, allowing for detailed surface topography imaging. Furthermore, to determine the chemical composition of the samples, EDS maps were acquired, with acquisition times of 30 minutes, and individual EDS spectra were recorded for 180 seconds per sample. In each case, ten spectra were acquired to ensure good averaging of the results.

SEM allows for the acquisition of surface images of samples with very high resolution, enabling detailed analysis of surface topography, particle shape, particle size, and any microstructures within the material. Images obtained by scanning electron microscopy provide the ability to identify potential defects, pores, cracks, and other characteristic structural features that may be significant in the context of material applications. Additionally, integration of energy dispersive X-ray spectroscopy (EDS) with SEM allows for real-time chemical analysis [24, 25].

Analysis of the specific surface area of stationary phases

The BET method (developed by Brunauer, Emmett, and Teller) is one of the most widely used techniques to determine the specific surface area of solid materials, including stationary phases used in liquid chromatography. It is based on the phenomenon of reversible adsorption of gas molecules on the surface of a solid, without the involvement of chemical bonding. The nitrogen is the most commonly used adsorbate, and measurements are typically performed at its liquefaction temperature (77 K), which allows the acquisition of a well-defined and reproducible adsorption isotherm. The aim of the BET method is to estimate the specific surface area, that is, the total surface area available for adsorption per unit mass of material (expressed in m^2/g). The determination of this value is based on the analysis of the nitrogen adsorption isotherm, a curve showing the amount of gas adsorbed by the sample as a function of the relative pressure P/P_0, where P denotes the working pressure and P_0 is the saturated vapor pressure of the adsorbate [26–28].

In the present study, the multipoint BET method was used for surface area analysis, which involves collecting data from several measurement points within the range of low relative pressures. It is assumed that adsorption occurs primarily through the formation of a monolayer of gas molecules on the surface of the material. Although the BET model also accounts for the possibility of multilayer adsorption, the key focus is on estimating the volume of the first monolayer, as this value serves as the basis for calculating the specific surface area. A linear form of the BET equation is used to determine the model parameters, and the resulting coefficients allow for the calculation of the volume of gas adsorbed in the monolayer. This value is then converted into surface area on the basis of known physical properties of the adsorbate, such as the surface area occupied by a single nitrogen molecule. The multipoint BET method, compared to the single-point BET version, is characterized by greater accuracy and resistance to errors resulting from imperfect data fitting. When multiple measurement points are incorporated, it is possible to more accurately reflect the actual course of the adsorption isotherm, which improves the reliability of the results, particularly for materials with heterogeneous surface morphology, irregular pores, or microporosity presence. The analysis of the specific surface area and the pore and volume size distribution was performed using the NOVA 1200e Surface Area & Pore Size Analyzer form Quantachrome INSTRUMENTS. The powder samples were vacuum degassed prior to analysis. The degassing lasted 2h for each sample. The degassing temperature was set at 250 °C. In the context of chromatographic studies, determining the specific surface area of the stationary phase not only enables comparison of the physicochemical properties of different materials, but also contributes to a better understanding of the retention mechanisms and intermolecular interactions the occur during the separation process [23, 29, 30].

Analysis of the pore volume and size distribution of stationary phases

Characterization of the porosity of adsorbents is an important step in evaluating their suitability as stationary phases in liquid chromatography. One of the most commonly used techniques for porosity analysis, particularly in the mesopore range, is the BJH method (i.e. the Barret-Joyner-Halenda method), which is based on the analysis of the nitrogen adsorption/desorption isotherm. This method uses the modified Kelvin equation to describe the phenomenon of capillary condensation occurring in cylindrical pores Equation 3. The main assumption of the BJH method is that during nitrogen adsorption, under specific pressure and temperature conditions, the adsorbate condenses in the pores, which allow its size to be estimated on the basis of changes in adsorbate volume. The applications of the Kelvin equation are presented in the available literature [e.g. 22, 31].

$$ln\frac{P}{P_0} = \frac{2\gamma V_M}{r_k RT} \quad (3)$$

where: $\frac{P}{P_0}$ – relative pressure, γ – surface tension of a liquid, V_M – molar volume of liquid nitrogen, r_k – capillary radius, R – gas constant, T – temperature in Kelvin (for liquid nitrogen 77 K) [22].

In the case of materials with irregular pore structures or complex morphology, the BJH method can lead to an underestimation of the micropore volume and errors in interpreting the pore distribution shape. This is particularly problematic when the pore structure is more complex than the simple cylindrical geometry assumed by this method. In such cases, traditional approaches may not fully account for the characteristics of pores with irregular shapes, leading to incorrect conclusions about the pore size and porosity of the material. To improve the accuracy of measurements in such cases, the BJH method is increasingly supplemented with advanced analysis based on density functional theory (DFT). This theory allows for the consideration of more complex interactions between adsorbate molecules and the pore walls. DFT enables the modeling of various pore geometries, such as slit-like, conical, or cylindrical, which allows for better reproduction of the actual adsorption conditions. Additionally, when the porosity of materials is evaluated, it is useful to calculate the average pore diameter (DH), which serves as an indicator of the general porosity properties of the materials. The average pore diameter is calculated as the ratio of four times the pore volume to the specific surface area of the material. Although this value is simplified and does not fully account for the complexity of the pore geometries, it provides a useful comparative parameter that enables a quick assessment of the porosity of the samples studied and can serve as a starting point for more advanced analyses [22, 32, 33]. Therefore, in the present study, the results of the BJH analysis were supplemented with an additional evaluation using DFT and the calculation of the average DH. This approach allowed for more precise information to be obtained regarding the porous structure of the materials.

RESULTS AND DISCUSSION

Microanalysis SEM-EDS of stationary phases

The results of the SEM-EDS analysis are presented in Table 2. The results showed that all of the adsorbents tested contain silicon and oxygen as dominant elements, indicating the presence of silica (SiO_2) as the primary base material of the stationary phases. The highest oxygen content (58.75%) was found for adsorbent D, suggesting possible differences in the surface modification process compared to other materials. A slightly lower oxygen content was observed for adsorbent A (58.33%). The lowest oxygen content (51.33%) was observed for adsorbent C, which may indicate a higher degree of hydrophobic modification. The chromium (Cr), iron (Fe), and nickel (Ni) were present in all samples but in trace amounts (below 5%). The highest iron content (3.28%) was found for adsorbent B, which could influence interactions with analytes containing functional groups that interact with metals. The nickel (Ni) content was similar between different samples (0.33–0.43%), but was highest for the adsorbent C (0.43%), which may be significant when analyzing substances susceptible to metallic catalysis.

Figure 1 shows the SEM-EDS and SEM-macro images of adsorbent A. The adsorbent is characterized by a fine-grained, irregular surface structure. Numerous micropores and indentations are visible, suggesting a relatively high specific surface area. This type of morphology is typical for stationary phases used in hydrophilic interaction chromatography (HILIC), where an

Table 2. Microanalysis of the stationary phases of the chromatographic columns studied

Chromatgraphic columns	Adsorbent designation	O (wt. %)	Si (wt. %)	Cr (wt. %)	Fe (wt. %)	Ni (wt. %)
TSK Gel Amide 80	A	58.33	37.64	0.70	2.96	0.35
Eurospher II 100-5 HILIC	B	56.41	39.12	0.778	3.28	0.398
Nucleodur C18 Gravity	C	51.33	44.23	0.783	3.22	0.43
Purospher STAR NH_2	D	58.75	37.49	0.67	2.75	0.33

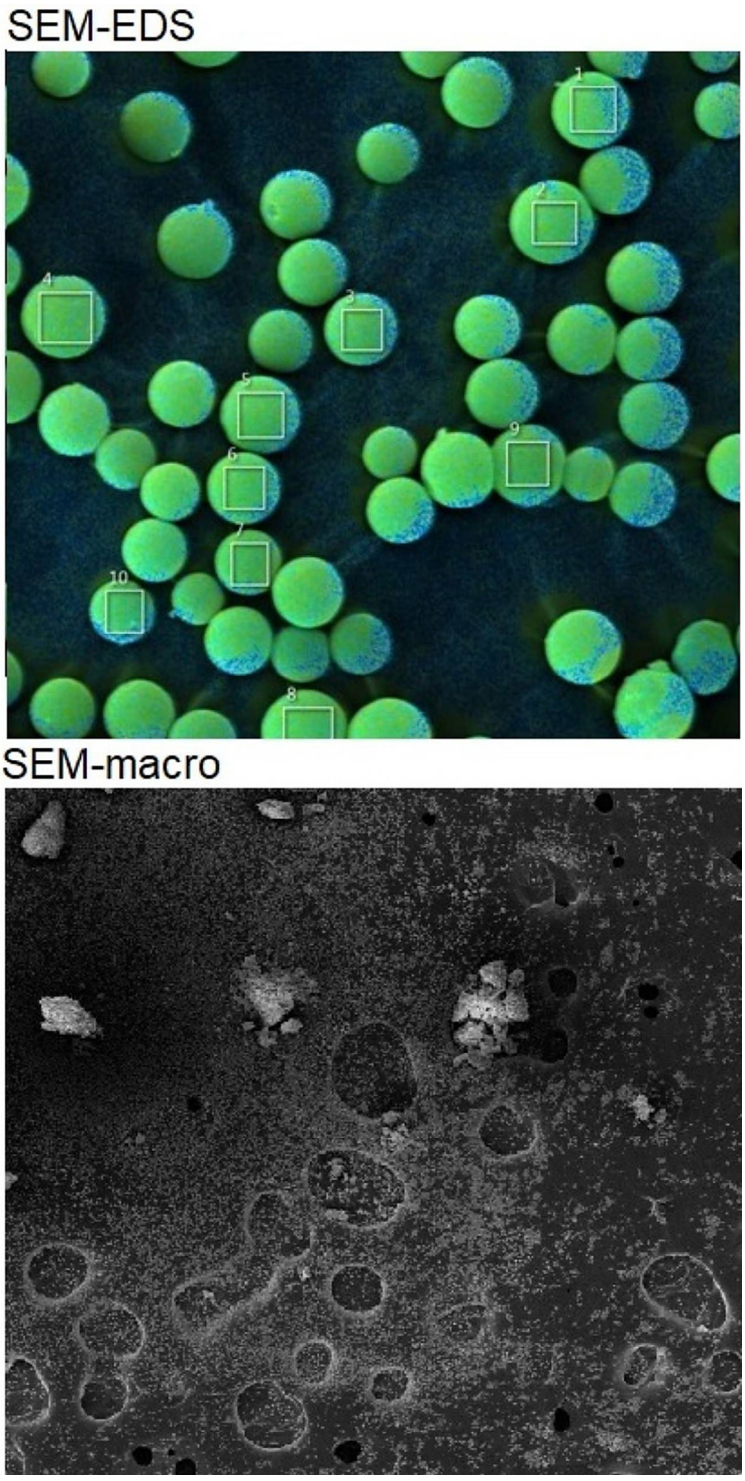

Figure 1. The SEM image with marked EDS analysis points and the SEM-macro image of the stationary phase from the TSK Gel Amide 80 chromatographic column

increased adsorption surface promotes the effective retention of polar analytes. There may also be a densification of surface-modifying particles, indicating strong hydrophilicity.

Figure 2 presents SEM-EDS and SEM-macro images of adsorbent B. Larger particle aggregates are visible, which may indicate heterogeneous surface modification. The presence of larger aggregates could affect the irregularity of the mobile phase flow and potentially lead to broad chromatographic peaks. As a results of the presence of larger structures, the material

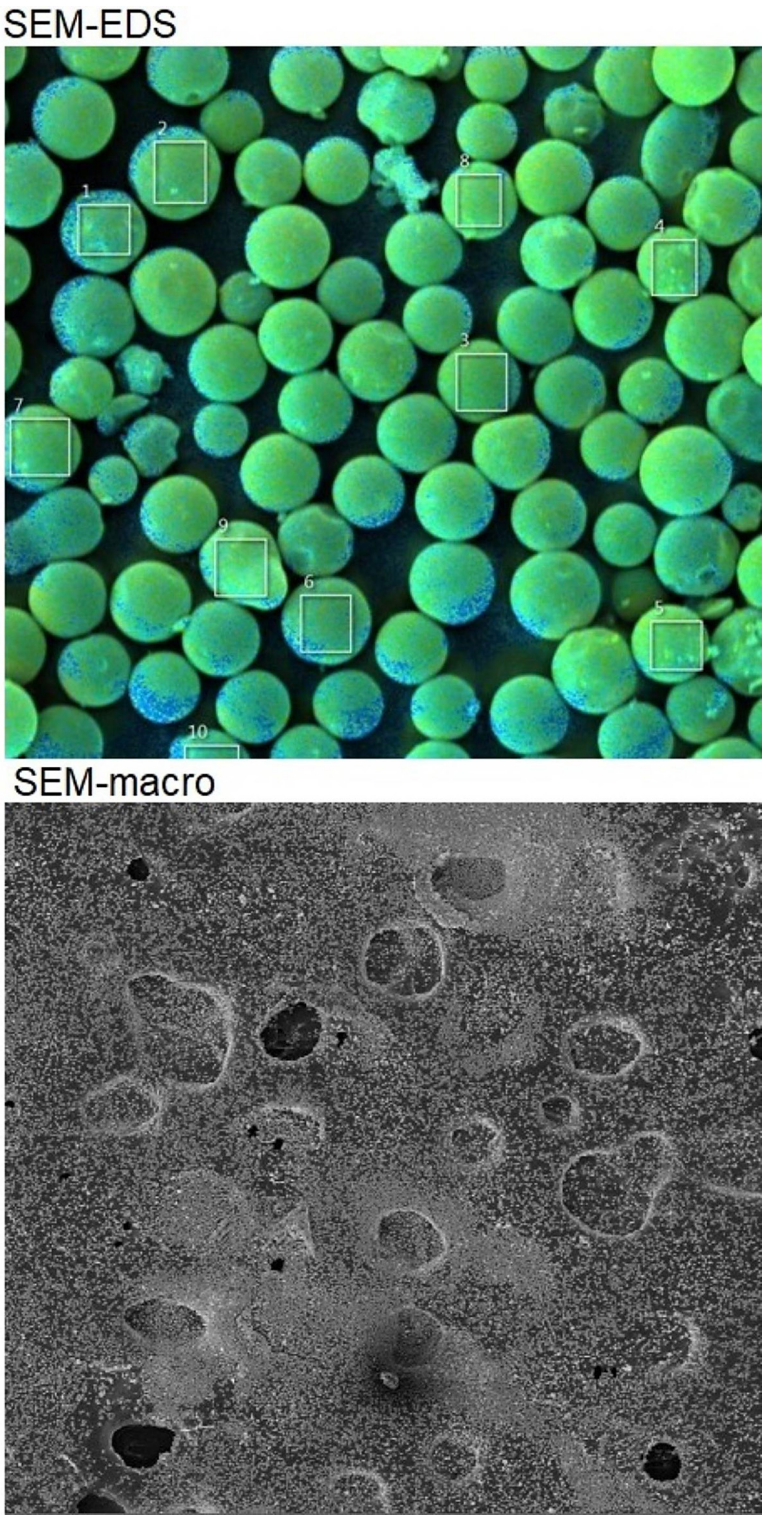

Figure 2. The SEM image with marked EDS analysis points and the SEM-macro image of the stationary phase from the Eurospher II 100-5 HILIC chromatographic column

may be more prone to clogging and may require proper sample preparation before analysis. The material likely has a highly developed porous microstructure, which may not be visible in the SEM images, as indicated by its high specific surface area.

Figure 3 shows the SEM-EDS and SEM-macro images of adsorbent C. The surface is relatively smooth. The absence of larger particle aggregates suggests uniform coverage with the hydrophobic phase C18. This structure is typical for reversed-phase (RP-HPLC) phases, where modification

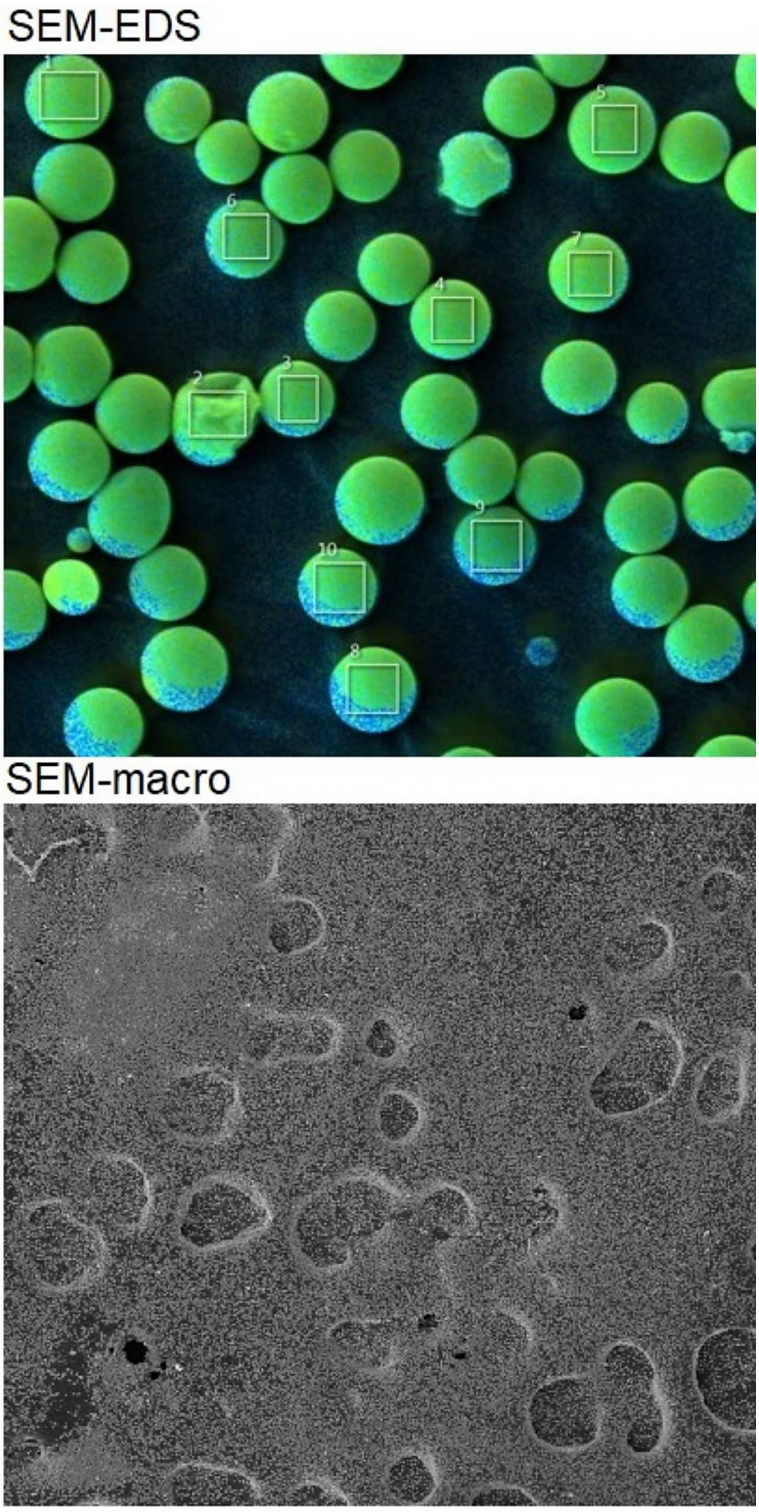

Figure 3. The SEM image with marked EDS analysis points and the SEM-macro image of the stationary phase from the Nucleodur C18 Gravity chromatographic column

with long hydrocarbon chains increases the material's hydrophobicity. The surface is denser than that in HILIC materials, which limits the adsorption of polar analytes. As a result, this material has a relatively low specific surface area compared to that of HILIC materials, which feature a more developed porous structure. The material is suitable for separating nonpolar and moderately polar analytes in reversed-phase chromatography. The lack of large pores may limit the adsorption of proteins and other large molecules.

Figure 4 shows the SEM-EDS and SEM-macro images of adsorbent D. The surface is moderately porous, with visible microchannels. The presence of recessed or fiber-like structures suggests uneven coverage of the surface with amine groups. The material may exhibit some ion-exchange properties, which is advantageous for the analysis of compounds with weak basic properties. The structure is somewhat less uniform than that of C18, which may affect the repeatability of the analyzes.

Analysis of the specific surface area of stationary phases – multipoint BET method

The specific surface area of the adsorbents was analyzed using the multipoint BET method for four different adsorbents designed as A, B, C, and D – see Table 1. The results were presented in Figures 5–8. Each of them has a different specific surface area, which is crucial in the context of their adsorption properties. The highest specific surface area value was obtained for adsorbent B, at 301.729 m^2/g, indicating that its high adsorption capacity and potentially higher efficiency in processes require a large surface available for adsorption. However, the smallest surface area was observed for adsorbent C, with a value of 162.554 m^2/g, which may suggest that its porous structure is less developed, resulting in lower adsorption capacity. The remaining two adsorbents A and D, achieved intermediate values of 256.39 m^2/g and 285.286 m^2/g, respectively, suggesting that their adsorption capacities are similar. The very high correlation coefficient for all samples, $R = 0.999$, indicates a strong agreement between the data and the multipoint BET model, meaning that this method effectively describes the adsorption properties of the studied materials.

A high specific surface area does not always indicate a good macroscopic structure – an example is adsorbent B: despite the aggregates, the internal structure provides a good surface for adsorption. The phase with a smooth surface (adsorbent C), has a clearly lower specific surface area – its main purpose is not polar adsorption, but the selective separation of nonpolar analytes.

The experimentally determined specific surface area values of the stationary phases varied significantly in some cases from those provided by the manufacturer (Table 3). For adsorbent A, the manufacturer declares a value of 450 m^2/g, while the result obtained using the multipoint BET method is 256.39 m^2/g. This is a very large discrepancy (193.61 m^2/g), suggesting that not all of the surface area declared by the manufacturer is actually available for nitrogen adsorption under multipoint BET conditions. The large deviation suggests that some of the surface area may be inaccessible to the gas in the BET analysis (e.g., pore clogging and chemical modification limiting accessibility). It is also possible that the method used by the manufacturer takes into account additional structural aspects that are not considered in the multipoint BET method. Multipoint BET analysis generally confirms good absorbency, but indicates that the material may not reach the full potential declared by the manufacturer. For adsorbent B, the manufacturer declared the value is 320 m^2/g, while the multipoint BET analysis showed 301.729 m^2/g, which resulting in a relatively small difference (18.27 m^2/g). This indicates that the manufacturer's data are largely consistent with the actual experimental results, suggesting that the pore structure of this column is fully utilized during adsorption. However, for adsorbent C, the manufacturer specifies a value of 338 m^2/g, while the multipoint BET method indicated 162.554 m^2/g, representing a significant difference of 175.446 m^2/g. This is the second largest discrepancy in the study, which may suggest that part of the surface area included in the manufacturer's declaration is not effectively available for nitrogen adsorption or that the pore structure does not allow for full utilization under multipoint BET measurement conditions. The SEM analysis confirms the experimental studies of the material's specific surface area. The surface is smooth and compact, resulting in low surface availability for adsorption. The hydrophobic modification C18 may "close" the pores, reducing the active surface area. The specific surface area for adsorbent D, according to the manufacturer, is 330 m^2/g, while the multipoint BET analysis

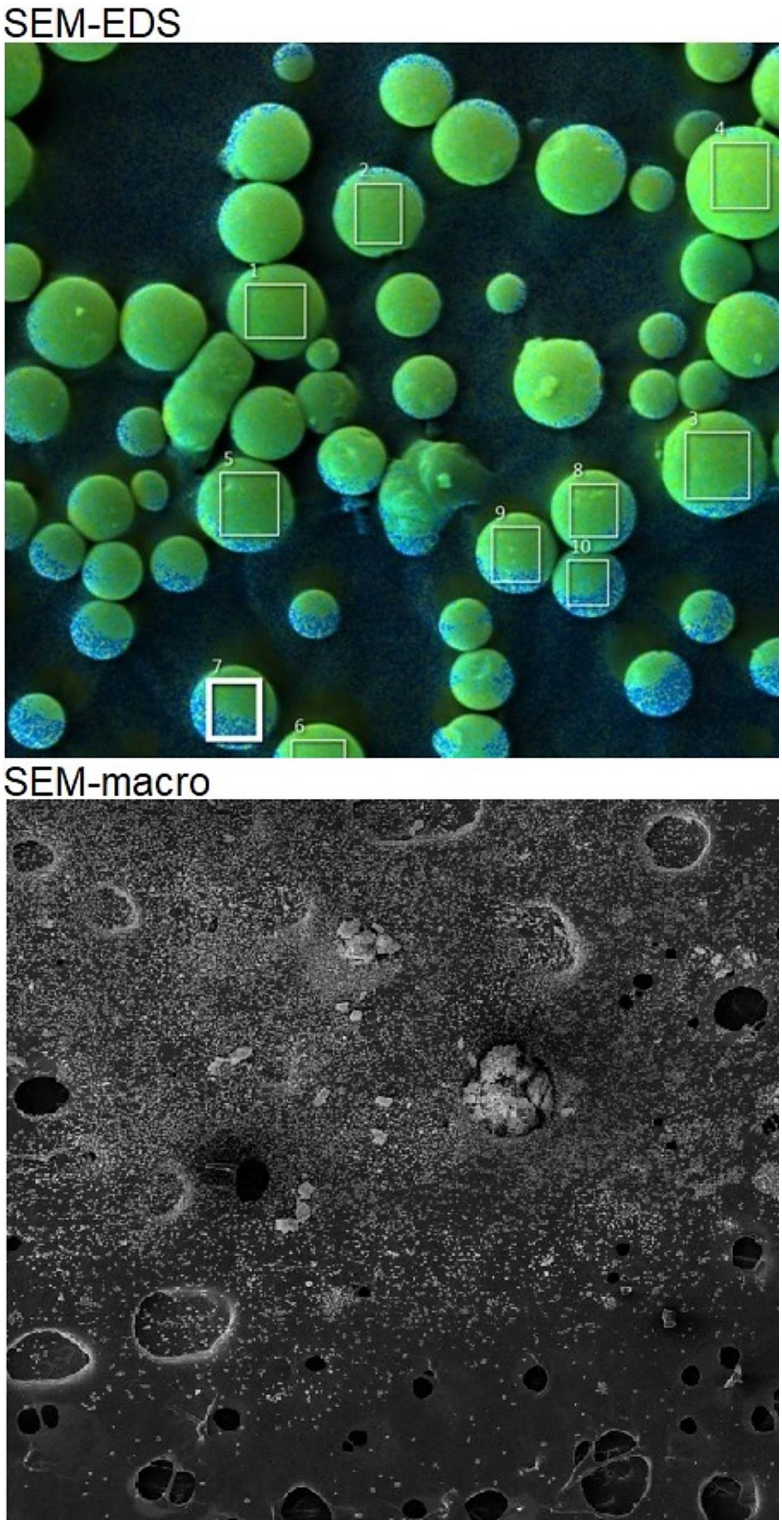

Figure 4. The SEM image with marked EDS analysis points and the SEM-macro image of the stationary phase from the Purospher STAR NH_2 chromatographic column

showed 285.286 m²/g. This means that the actual specific surface area is about 44.7 m²/g smaller, which may indicate differences arising from the measurement methodology or the degree of pore accessibility under actual adsorption conditions.

Analysis of the pore volume and size distribution of stationary phases

Porosity characterization is an important factor in assessing the suitability of stationary phases used in liquid chromatography, because it directly

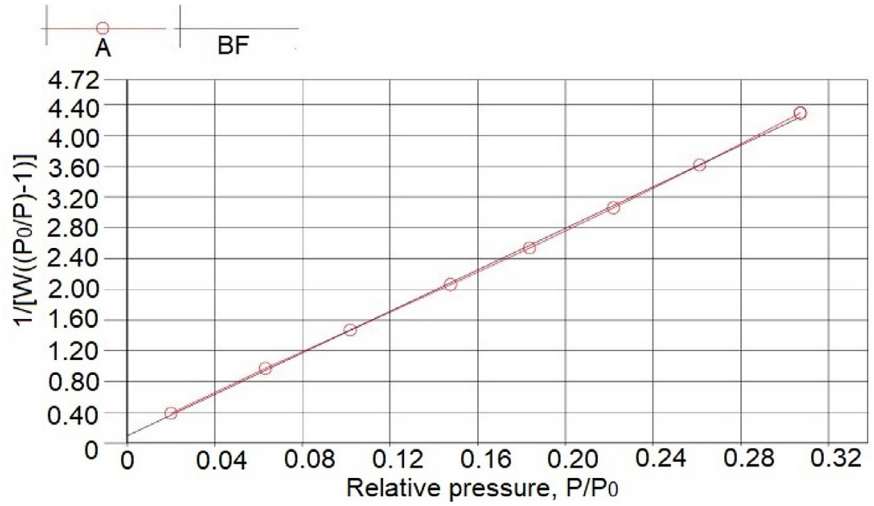

Figure 5. The multipoint BET plot for the stationary phase of the TSK Gel Amide 80 chromatographic column

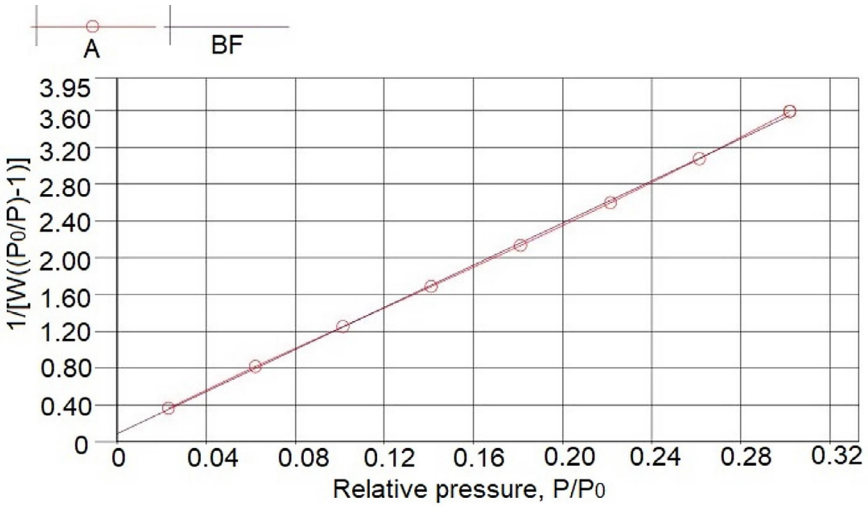

Figure 6. The multipoint BET plot for the stationary phase of the Eurospher II 100-5 HILIC chromatographic column

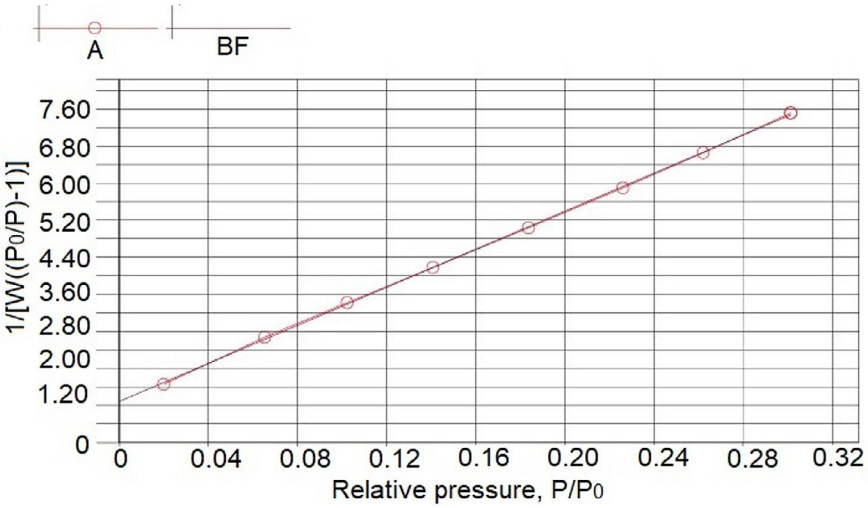

Figure 7. The multipoint BET plot for the stationary phase of the Nucleodur C18 Gravity chromatographic column

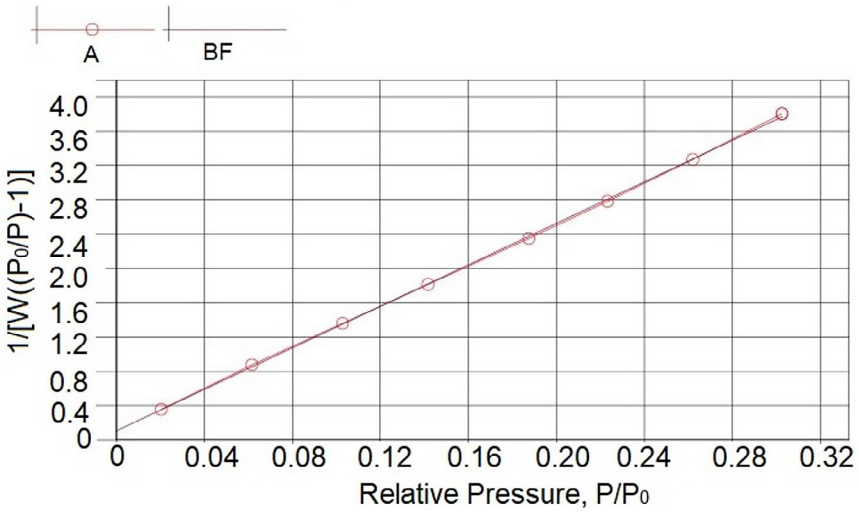

Figure 8. The multipoint BET plot for the stationary phase of the Purospher STAR NH_2 chromatographic column

Table 3. The specific surface area of adsorbents: comparison of experimental results with manufacturer data

Stationary phase	Adsorbent designation	Surface area (m^2/g) - experimental results	Surface area (m^2/g) - declared by the manufacturer	Percentage variation (%)
TSK Gel Amide 80	A	256.39	450	43.0
Eurospher II 100-5 HILIC	B	301.729	320	5.7
Nucleodur C18 Gravity	C	162.554	338	51.9
Purospher STAR NH_2	D	285.286	330	13.5

influences the accessibility of the surface area of analytes and the efficiency of retention processes. In this study, a detailed analysis of four different chromatographic materials presented in Table 1 was performed. The pore size distribution and pore volume were determined using BJH, DH, and DFT methods based on nitrogen adsorption and desorption isotherms.

The graphs (Figures 9–12) presenting the results of the BJH analysis show two dependencies: *V* – the cumulative pore volume (cc/g) on the left Y-axis and *dV(logr)* – the differential pore volume distribution with respect to the logarithm of the pore radius on the right Y-axis. The X-axis represents the pore radius expressed in [Å]. Using a logarithmic scale for the radius ("*logr*") allows for a more precise and clearer interpretation of the pore size distribution across a wide range of pore sizes.

The stationary phase A is characterized by an average pore diameter is approximately 59.49–69.06 Å, determined by the BJH and DH methods, while the DFT method indicates a slightly smaller value of 44.61 Å (Table 4). This indicates the presence of mesopores, that is, pores with diameters in the range of 2 to 50 nm. The high consistency of the results obtained by the BJH and DH methods confirms the stability of the pore size distribution and the absence of significant errors arising from model assumptions. The pore volume of this phase is also relatively high (0.71–0.75 cc/g), indicating a large available space for adsorbate molecules. This type of structure can be beneficial for the separation of compounds with larger molecular sizes, offering a balance between the pore accessibility and interaction surface area. The adsorption and desorption profiles (Fig. 9) suggest the presence of an ordered network of medium-size pores. The adsorption isotherm shows an increasing volume of adsorbed nitrogen with increasing relative pressure. The shape of the isotherm indicates the presence of mesopores with a relatively homogeneous size distribution.

The stationary phase B differs significantly in terms of pore properties. The average pore diameter is approximately 15.9–16.3 Å, while the DFT method gives a value of 7.713 Å, which clearly classifies this material as microporous (< 2 nm). The pore volume ranges from 0.42 to 0.47 cc/g (Table 4). Such small pores limit the availability of internal surface area for larger molecules, which may affect the retention of analytes in liquid chromatography. At the same time, this structure

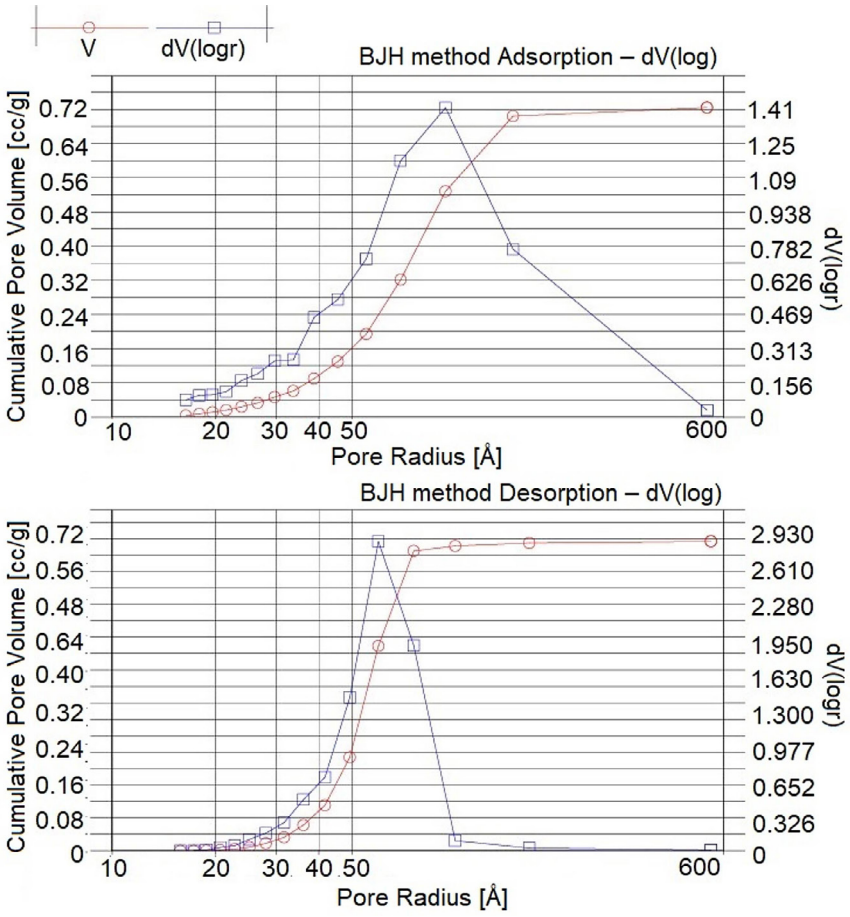

Figure 9. The BJH method adsorption/desorption plot for stationary phase of the TSK Gel Amide 80 chromatographic column

favors selective molecular interactions, particularly with small and strongly polar compounds. The adsorption curve (Figure 10) shows a less steep adsorption curve compared to adsorbent A. The gradual increase in the volume of adsorbed gas suggests a diversity in the pore sizes. In the case of desorption, a more pronounced hysteresis is observed compared to the previous adsorbent, which may indicate a pore structure with an irregular shape. This suggests a greater difficulty in removing adsorbed molecules, which may influence chromatographic applications.

The stationary phase C exhibits intermediate porous properties – the diameter of the pore is approximately 23.80–41.6 Å by the BJH and DH methods, while using the DFT method approximately 38.98 Å (Table 4). This may indicate the presence of a more complex pore morphology or effects related to the averaging of pore profiles in different mathematical models. The pore volume ranges from 0.37 to 0.40 cc/g. Such a porous structure is typical for reverse phase phases and allows for effective separation of compounds with varied polarity and size. In the case of adsorption (Figure 11), a very characteristic and more vertical isotherm profile suggests the presence of well-defined mesopores. Sharp adsorption within a specific pressure range indicates a porosity optimized for selective adsorption. On the contrary, the hysteresis observed during desorption is smaller than that for the stationary phase B, suggesting a more regular pore structure.

The highest values for both pore diameter and volume were recorded for the adsorbent D. The diameter of the pores reaches as high as 76.1 to 93.3 Å (BJH and DH methods), and 53.41 Å using the DFT method (Table 4). These values are characteristic of strongly mesoporous materials with a tendency toward macroporosity. The pore volume exceeds 1.1 cc/g, making this phase the most porous among the analyzed materials. Such a structure may be significant in the context of large molecule retention, as well as in the presence of a reaction affecting the mass transfer rate and the

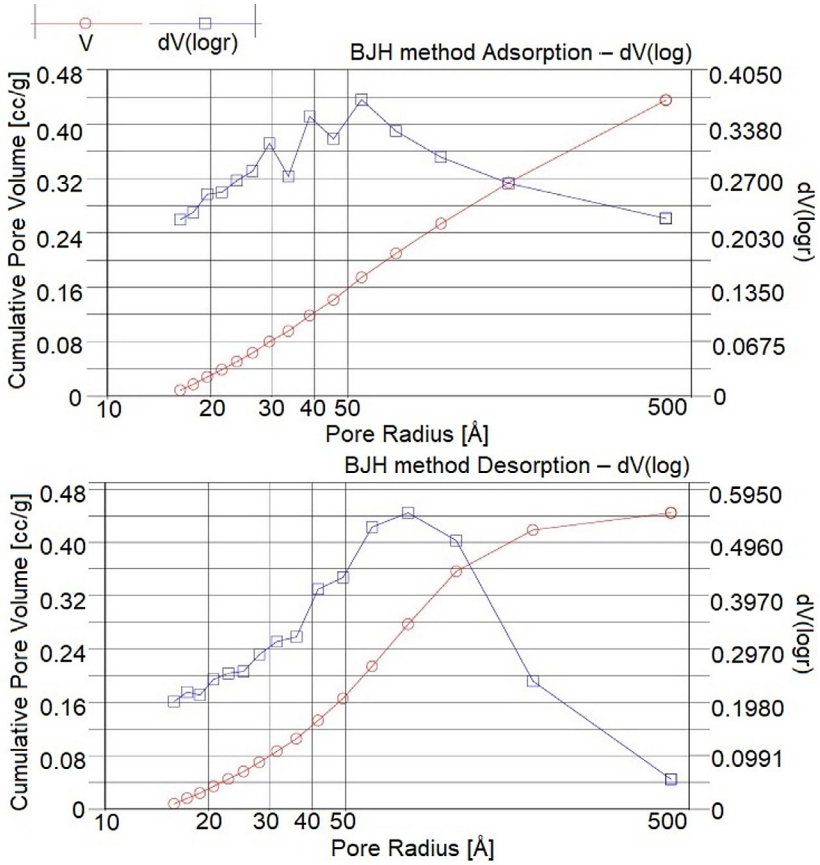

Figure 10. The BJH method adsorption/desorption plot for stationary phase of the Eurospher II 100-5 HILIC chromatographic column

Table 4. The pore volume and size distributions for stationary phases of the chromatographic columns

Pore size distribution					
Stationary phase	Adsorption		Desorption		DFT [Å]
	BJH [Å]	DH [Å]	BJH [Å]	DH [Å]	
A (TSK Gel Amide 80)	69.06	69.06	59.49	59.49	44.61
B (Eurospher II 100-5 HILIC)	16.29	16.29	15.87	15.87	7.71
C (Nucleodur C18 Gravity)	23.80	23.80	41.62	41.62	38.98
D (Purospher STAR NH_2)	93.38	93.38	76.09	76.09	53.41
Volume size distribution					
Stationary phase	Adsorption		Desorption		DFT [cc/g]
	BJH [cc/g]	DH [cc/g]	BJH [cc/g]	DH [cc/g]	
A (TSK Gel Amide 80)	0.7246	0.7077	0.7537	0.7364	0.7338
B (Eurospher II 100-5 HILIC)	0.4356	0.4251	0.4440	0.4337	0.4735
C (Nucleodur C18 Gravity)	0.3856	0.3764	0.3972	0.3880	0.3769
D (Purospher STAR NH_2)	1.1450	1.1170	1.1890	1.1610	1.1400

volume of separated pores. High porosity may also result in greater retention of the mobile phase, which should be considered when selecting chromatographic conditions. In the case of adsorption (Figure 12), the adsorption profile shows a wide range of porosity, suggesting the presence of both mesopores and potentially micropores. The gradual increase in adsorption without a distinct plateau phase indicates a diverse surface structure. In contrast, during desorption, the largest hysteresis among all of the analyzed adsorbents is observed, which indicates a complex pore structure.

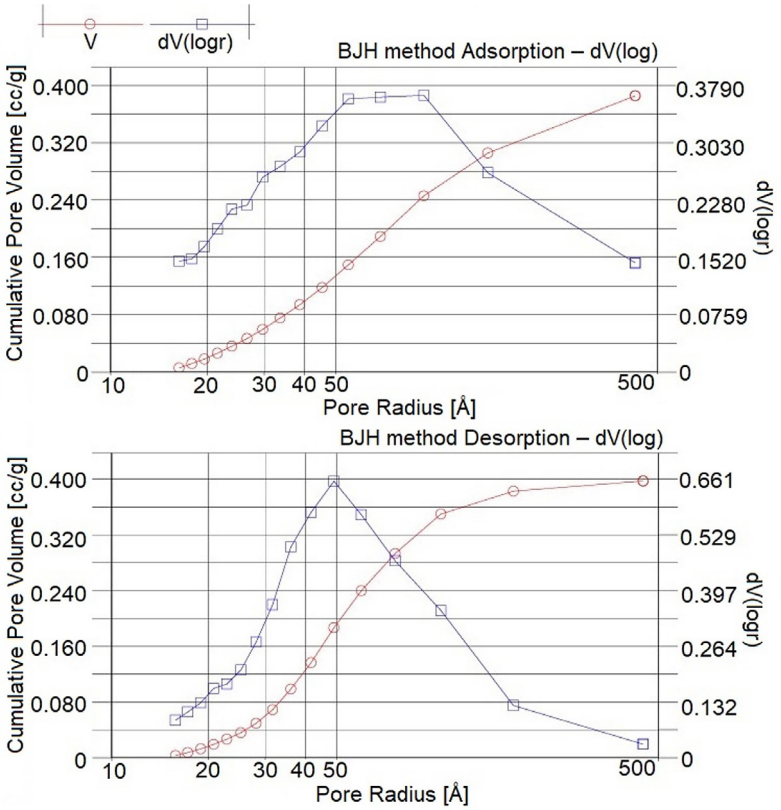

Figure 11. The BJH method adsorption/desorption plot for stationary phase of the Nucleodur C18 Gravity chromatographic column

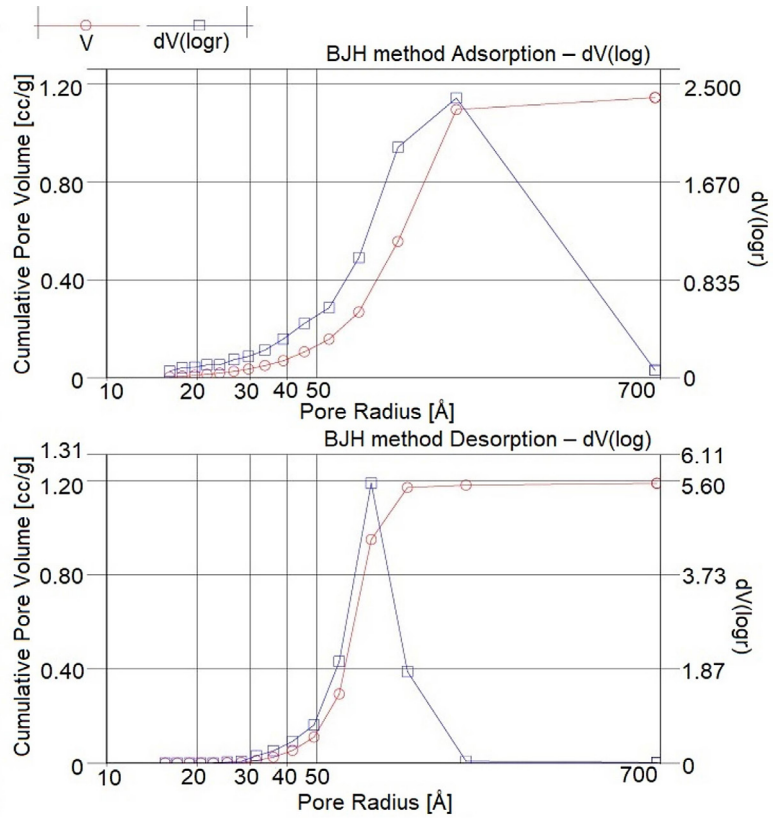

Figure 12. The BJH method adsorption/desorption plot for stationary phase of the Purospher STAR NH_2 chromatographic column

CONCLUSIONS

Based on SEM-EDS analyzes of the chromatographic column adsorbents, it can be concluded that all materials contain silica (SiO_2) as the main component, which is typical for stationary phases used in chromatography. Differences in oxygen content between materials indicate varying surface modification processes. Specifically, the high oxygen content in the TSK Gel Amide 80 adsorbent suggests a strong hydrophilic modification, which promote effective retention of polar analytes, while the lower oxygen content in the Nucleodur C18 Gravity adsorbent indicates a higher degree of hydrophobic modification, which is beneficial for the separation of nonpolar analytes. The Purospher STAR NH_2 adsorbent was also shown to have an oxygen content similar to the TSK Gel Amide 80 adsorbent, indicating the presence of functional groups associated with surface modification. Furthermore, the presence of metals such as iron and nickel, although in trace amounts, may influence interactions with certain analytes, especially those reacting with metals. The analyzed materials exhibit a variety of surface structures that directly affect their adsorption properties. The columns with stationary phases having a more uniform surface, such as C18, are more effective in separating nonpolar analytes, while materials such as the TSK Gel Amide 80 stationary phase, due to their porosity and higher specific surface area, perform better in hydrophilic interaction chromatography. These conclusions highlight the importance of selecting the appropriate stationary phases according to the characteristics of the analyzed samples and the chromatographic requirements.

The results of the specific surface area measurements using the multipoint BET method for the studied chromatographic column adsorbents showed significant discrepancies compared to the data declared by the manufacturers for some stationary phases. The largest discrepancy was observed for the TSK Gel Amide 80 and Nucleodur C18 Gravity adsorbents, while for other adsorbents such as Eurospher II 100-5 HILIC and Purospher STAR NH_2, the differences were smaller, suggesting a better agreement with the manufacturers data declared. Such large differences in the specific surface area results may indicate differences in pore accessibility under measurement conditions, as well as the use of different methodologies or additional structural aspects by the manufacturers that are not accounted for in the standard multipoint BET method. These findings emphasize the need for more precise specific surface area measurements, considering pore accessibility under actual analytical conditions.

The comparison of all stationary phases shows that their porous structures differ and may have a substantial impact on the separation mechanisms used in liquid chromatography. The TSK Gel Amide 80 phase features a mesoporous structure with a pore diameter of approximately ~44–69 Å (depending on the method) and a relatively large pore volume (0.71–0.75 cc/g). The uniform pore distribution and the presence of hysteresis indicate a stable structure, favorable for the separation of larger molecules, because of balanced access to the sorptive surface. The Eurospher II 100-5 HILIC adsorbent exhibits a distinctive microporous character, with pore diameters ranging from ~7–16 Å and the pore volume (0.42 to 0.47 cc/g). This structure promotes selective interactions with small and polar analytes but may limit efficiency for larger molecules. Hysteresis suggests an irregular pore structure and potentially more difficult desorption. The stationary phase of the Nucleodur C18 Gravity has an average porosity, with a varied pore diameter from ~24 to 42 Å (depending on the method) and moderate pore volume (0.38 to 0.40 cc/g). Its properties are typical for reversed phase materials, making it versatile in chromatographic applications. The regular pore structure and small hysteresis favor efficient flow and easy desorption. The stationary phase of Purospher STAR NH_2 is notable for having the highest porosity, with a diameter of the pores reaching up to 93 Å and volume of pores greater than 1.1 cc/g. These properties may indicate the presence of macropores and a highly diverse pore structure. While this facilitates the analysis of large molecules and rapid mass transfer, it also increases the risk of retention of analytes and affects prolonged desorption.

Acknowledgments

Financed by the Minister of Science and Higher Education Republic of Poland within the program "Regional Excellence Initiative", agreement no. RID/SP/0032/2024/01.

REFERENCES

1. Ali A.H. High-Performance Liquid Chromatography (HPLC): A review. HSPI Ann Adv Chem. 2022; 6: 10–20, https://doi.org/10.29328/journal.aac.1001026
2. Fekete S., Kohler I., Rudaz S., Guillarme D. Importance of instrumentation for fast liquid chromatography in pharmaceutical analysis. J. Pharm. Biomed. Anal. 2014; 87: 105–119, http://dx.doi.org/10.1016/j.jpba.2013.03.012
3. Unger K.K., Liapis A.I. Adsorbents and columns in analytical high-performance liquid chromatography: Aperspective with regard to development and understanding. J. Sep. Sci. 2012; 35(10–11): 1201–1212, https://doi.org/10.1002/jssc.201200042
4. Chavan R.V., Kengar M.D., Dhole A.R., Salunkhe V.R. A review on adsorbents in chromatography. IJSRST 2019; 6(3): 2395–6011, https://doi.org/10.32628/IJSRST19636
5. Zhao L.,Qin H., Wu R., Zou H. Recent advances of mesoporous materials in sample preparation. J. Chromatogr. A 2012; 1228:193-204, https://doi.org/10.1016/j.chroma.2011.09.051
6. Jaćkowska M., Bocian Sz., Gawdzik B., Grochowicz M., Buszewski B. Influence of chemical modification on the porous structure of polymeric adsorbents. Materials Chem. Phys. 2011; 130(1–2): 644–650, https://doi.org/10.1016/j.matchemphys.2011.07.039
7. Liu W., Zhang Y.,Wang S., Bai l., Deng Y., Tao J. Effect of pore size distribution and amination on adsorption capacities of polymeric adsorbents. 2021; 26: 5267, https://doi.org/10.3390/molecules26175267
8. Godinho J.M., Naese J.A., Toler A.E., Boyes B.E., Henry R.A., DeStefano J.J., Grinias J.P. Importance of particle pore size in determining retention and selectivity in reversed phase liquid chromatography. J. Chromatogr. A 2020; 1634: 461678, https://doi.org/10.1016/j.chroma.2020.461678
9. Ongkudon C.M., Kansil T., Wong C. Challenges and strategies in the preparation of large-volume polymer-based monolithic chromatography adsorbents.J. Sep. Sci. 2014; 37(5): 455–464, https://doi.org/10.1002/jssc.201300995
10. Gritti F., Guiochon G. Mass transfer kinetics, band broadening and column efficiency. J. Chromatogr. A 2012; 1221:2-40, https://doi.org/10.1016/j.chroma.2011.04.058
11. Gritti F., Guiochon G. New insights on mass transfer kinetics in chromatography. AIChE Journal. 2011; 57(2): 333–345, https://doi.org/10.1002/aic.12271
12. Gritti F., Guiochon G. The mass transfer kinetics in columns packed with Halo-ES shell particles. J. Chromatogr. A 2011; 1218(7): 907–921, https://doi.org/10.1016/j.chroma.2010.12.046
13. Gritti F., Guiochon G. Importance of sample intraparticle diffusivity in investigations of the mass transfer mechanism in liquid chromatography. AIChE Journal 2011; 57(2): 346–358, https://doi.org/10.1002/aic.12280
14. Broeckhoven K., Desmet G. Methods to determine the kinetic performance limit of contemporary chromatographic techniques. J. Sep. Sci. 2021; 44(1): 323–339, https://doi.org/10.1002/jssc.202000779
15. Gritti F., Guiochon G. Perspectives on the evolution of the column efficiency in liquid chromatography. Anal. Chem. 2013; 85(6): 3017–3025, https://doi.org/10.1021/ac3033307
16. Rastegar S.O., Gu T. Empirical correlations for axial dispersion coefficient and Peclet number in fixed-bed columns. J. Chromatogr. A 2017; 1490: 133–137, https://doi.org/10.1016/j.chroma.2017.02.026
17. Gritti F., McDonald T., Gilar M. Accurate measurement of dispersion data through short and narrow tubes used in very high-pressure liquid chromatography. J. Chromatogr. A 2015; 1410: 118–128, http://dx.doi.org/10.1016/j.chroma.2015.07.086
18. Antos D., Kaczmarski K., Piątkowski W. Preparative chromatography as a process of mixtures separation. WNT Warszawa 2011.
19. Lee D.W., Yoo B.R. Advanced silica/polymer composites: Materials and applications. J. Ind. Eng. Chem. 2016; 38: 1–12, https://doi.org/10.1016/j.jiec.2016.04.016
20. Manyangadze M., Chikuruwo N.H.M., Chakra C.S., Narsaiah T.B., Radhakumari M., Danha G. Enhancing adsorption capacity of nano-adsorbents via surface modification : a review. S. Afr. J. Chem. Eng.2020; 31(1): 25–32, https://doi.org/10.1016/j.sajce.2019.11.003
21. Cossio R., Albonico C., Zanella A., Fraterrigo-Garofalo S., Avataneo C., Compagnoni R.,TurciF. Innovative unattended SEM-EDS analysis for asbestos fiber quantification, Talanta, 2018; 190: 158–166, https://doi.org/10.1016/j.talanta.2018.07.083
22. Bardestani R., Patience G.S., Kaliaguine S. Experimental methods in chemical engineering: specific surface area and pore size distribution measurements—BET, BJH, and DFT. J. Chem. Eng. 2019; 97(11): 2781–2791, https://doi.org/10.1002/cjce.23632
23. ShamsiJazeyi H., Verduzco R., Hirasaki G.J. Reducing adsorption of anionic surfactant for enhanced oil recovery: Part I. Physicochem. Eng. Aspects 2014; 453: 162–167, http://dx.doi.org/10.1016/j.colsurfa.2013.10.042
24. Moro D., Ulian G., Valdrè G. SEM-EDS nanoanalysis of mineral composite materials: A Monte Carlo approach. Compos. Struct. 2021; 259: 113227, https://doi.org/10.1016/j.compstruct.2020.113227

25. Moro D., Ulian G., Valdrè G. Monte Carlo strategy for SEM-EDS micro-nanoanalysis of geopolymer composites, Compos. Part C 2021; 6: 100183, https://doi.org/10.1016/j.jcomc.2021.100183
26. Shimizu S., Matubayasi N. Surface area estimation: replacing the Brunauer−Emmett−Teller model with the statistical thermodynamic fluctuation theory. Langmuir 2022; 38(26): 7989−8002, https://doi.org/10.1021/acs.langmuir.2c00753
27. Khan A.S.A. Theory of adsorption equilibria analysis based on general equilibrium constant expression. Turk. J. Chem. 2012; 36(2): 219–231, https://doi.org/10.3906/kim-1110-6
28. Galarneau A., Mehlhorn D., Guenneau F., Coasne B., Villemot F., Minoux D., Aquino C., Dath J.P. Specific surface area determination for microporous/mesoporous materials: the case of mesoporous FAU-Y zeolites. Langmuir 2018; 34(47): 14134−14142, https://doi.org/10.1021/acs.langmuir.8b02144
29. Ma X., Li J., Rankin M.A., Croll L.M., Dahn J.R. Highly porous MnO_x prepared from $Mn(C_2O_4)\cdot 3H_2O$ as an adsorbent for the removal of SO_2 and NH_3. Microporous Mesoporous Mater. 2017; 244: 192–198, https://doi.org/10.1016/j.micromeso.2016.10.019
30. Hayati-Ashtiani M. Characterization of nanoporous bentonite (montmorillonite) particles using FTIR and BET-BJH analyses.Part. Part. Syst. Charact. 2011; 28(3–4): 71–76, https://doi.org/10.1002/ppsc.201100030
31. Haghighatju F., Rafsanjani H.H., Esmaeilzadeh F. Estimation of the dimension of micropores and mesopores in single walled carbon nanotubes using the method Horvath–Kawazoe, Saito and Foley and BJH equations. Micro & Nano Letters 2017; 12(1): 1–5, https://doi.org/10.1049/mnl.2016.0306
32. Tan Y.H., Davis J.A., Fujikawa K., Ganesh N.V., Demchenko A.V., Stine K.J. Surface area and pore size characteristics of nanoporous gold subjected to thermal, mechanical, or surface modification studied using gas adsorption isotherms, cyclic voltammetry, thermogravimetric analysis, and scanning electron microscopy. J. Mater. Chem. 2012; 22(14): 6733–6745, https://doi.org/10.1039/C2JM16633J
33. Landers J., Gor G.Y., Neimark A.V. Density functional theory methods for characterization of porous materials. Colloids Surf. A 2013; 437: 3–32, https://doi.org/10.1016/j.colsurfa.2013.01.007